Chemical Engineering Journal 152 (2009) 556–565

Contents lists available at ScienceDirect

Chemical Engineering Journal

journal homepage: www.elsevier.com/locate/cej

Model-free kinetic analysis of melamine–formaldehyde resin cure

A. Kandelbauer[a,*], G. Wuzella[b], A. Mahendran[b], I. Taudes[b], P. Widsten[b]

[a] Department of Wood Science and Technology, University of Natural Resources and Applied Life Sciences, Peter Jordan Strasse 82, A-1190 Vienna, Austria
[b] WOOD Carinthian Competence Centre, Kompetenzzentrum Holz GmbH, Klagenfurterstrasse 87 – 89, A-9300 St. Veit an der Glan, Austria

ARTICLE INFO

Article history:
Received 15 December 2008
Received in revised form 12 May 2009
Accepted 18 May 2009

Keywords:
Melamine–formaldehyde resin
Kinetics
Isoconversional kinetics
Curing
Differential scanning calorimetry

ABSTRACT

The curing behaviour of an industrial melamine–formaldehyde (MF) resin with four different commercial curing catalysts was analyzed from thermal studies using differential scanning calorimetry (DSC) and model-free kinetic (MFK) analysis. For the kinetic study, the mathematical approaches developed by Friedman, Flynn–Wall–Ozawa, Kissinger–Akahira–Sunose and Vyazovkin were used to calculate curing isotherms. With all kinetic approaches the apparent activation energy, E_a, depended to some extent on the degree of conversion (α). Besides being obscured by experimental errors, in some cases higher $E_a(\alpha)$ were calculated with higher catalyst concentrations, illustrating that $E_a(\alpha)$ may not be the only relevant parameter to compare different resin systems. However, $E_a(\alpha)$ was found to be well suited for predicting the isothermal curing behaviour of MF resin. The time required for achieving a certain conversion, α, was calculated for different temperatures. By comparing the calculated isotherms to experimental isothermal data obtained at 80, 100, and 120 °C it was found that the Vyazovkin approach in its advanced form was best suited to predict the curing kinetics of MF with all catalyst systems tested. By applying DSC–MFK it was possible to detect and characterize the de-blocking behaviour of different catalysts for MF curing. The presented results illustrate that isoconversional methods for kinetic analysis of thermochemical data can be applied to the investigation and optimization of melamine–formaldehyde resins.

1. Introduction

Products containing melamine-based aminoplastic resins are present in our daily environment, for example, as furniture, flooring, or exterior cladding, and represent an important market segment. Approximately 1 million metric tons of melamine was consumed in 2006; for 2009, the consumption is estimated to reach 1.3 million tons [1]. The major consumers of melamine are the wood-based panel and laminate manufacturers, which supply the furniture and construction industries with high-quality surface-coated interior and exterior materials [1]. Typically, particleboards are manufactured by gluing comminuted lignocellulosic material with 20–25% (w/w) of a melamine–formaldehyde (MF) resin in a hot press [2]. Practically all of these boards are subsequently coated with sheets of decorative paper that are impregnated with MF resins to obtain wood-like or custom design surfaces [3]. While about 30% of the melamine produced in 2006 was consumed in the manufacture of wood adhesives, the largest proportion was used for MF impregnation and coating resins for industrial laminates (ca. 50%). The remainder went to surface coatings (9%), moulding compounds (7%), and other applications [1].

The curing behaviour of an MF resin and its degree of cross-linking govern the customized product properties. If the resin is not sufficiently cured, particleboards glued with MF will lack mechanical strength [4] and surface finishes based on MF-impregnated papers will lack hardness, durability, brilliance, and resistance towards hydrolysis and chemical agents [5]. The cost of particleboard manufacturing is mainly governed by the production line speed so that the reaction time required for a specific cross-linking degree of MF is an important issue. Lamination of impregnated sheets onto wood-based panels takes place in presses at temperatures between 160 and 180 °C. Depending on the type of product, the pressurized cycle times of modern press equipment range from 6 to 30 s for short-cycle presses to several minutes in multi-platen presses. The supplier of impregnated paper must be able to deliver products suitable for the whole variety of different pressing conditions used by his customers. In short, for the whole range of products in the wood-based panel industry, a rapid achievement of an optimal cross-linking degree upon pressing is desired and resin technologists need to know how to design gluing formulations and impregnation solutions complying with product properties, production technology, and production speed.

A key issue in tailoring the curing behaviour of MF resins is the right choice of type and amount of curing catalyst [6]. To obtain the desired product properties in the shortest time possible, it must be known what degree of cross-linking (α) can be obtained with a

* Corresponding author. Tel.: +43 4212 494 8002; fax: +43 4212 494 8099.
E-mail address: andreas.kandelbauer@boku.ac.at (A. Kandelbauer).

1385-8947/$ – see front matter © 2009 Elsevier B.V. All rights reserved.
doi:10.1016/j.cej.2009.05.027

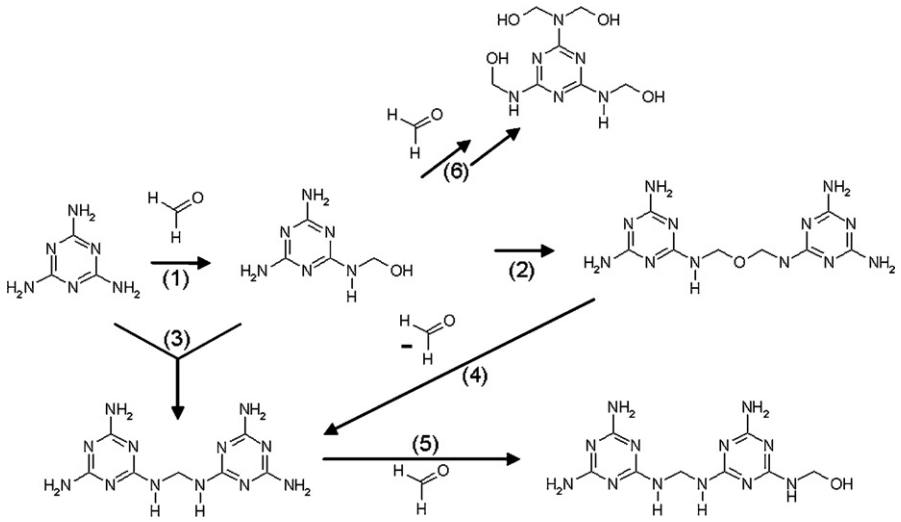

Fig. 1. Schematic representation of some elementary reactions taking place during the initial phase of melamine–formaldehyde resin condensation: (1, 5, 6) methylolation, (2) formation of methylene-ether bridges, (3) formation of methylene bridges, and (4) rearrangement with formaldehyde liberation.

certain combination of MF and curing catalyst at a specified cure time and temperature. While classical reaction kinetics can supply this information for reactions where the reaction mechanisms are known and quantitative relationships between the reactants and products can be accurately formulated, such information is not available for the cross-linking of MF resins. Although the elementary MF cross-linking reactions are known, the reaction mechanism is rather complex and cannot be used accurately for quantitative predictions. This is illustrated in Fig. 1.

MF resin formation proceeds in two steps [2]. Initially, melamine is amino-methylolated by addition of formaldehyde (Fig. 1, (1)). Depending on the molar ratio and the reaction conditions, the degree of methylolation ranges from one to six (Fig. 1, (6)). In the second step, condensation takes place and basically two types of bridges are formed. Methylene-ether bridges (Fig. 1, (2)) are formed by auto-condensation of two methylol groups. Amino-methylene bridges (Fig. 1, (3)) result from condensation of methylol compounds with free amino groups present on the triazine ring [7]. Formaldehyde addition is reversible and structural rearrangements are observed [8]. Upon hydrolysis of methylene ether bonds, formaldehyde may be re-liberated (Fig. 1, (4)) and is thus available for introducing cross-linking sites at different positions (Fig. 1, (5)). The numerous possibilities for recombination of the various chemical species lead to very complex reaction mixtures especially if modifying chemicals such as urea are co-polymerized into the melamine–formaldehyde network [9,10] in the case of wood binder resins. The condensation strongly depends on reaction parameters such as molar ratio, pH, and temperature profiles during resin preparation [7]. The system is further complicated by incorporation of different types of additives and curing catalysts, and classic kinetic models for describing the curing kinetics are bound to fail due to the lack of knowledge of an appropriate mechanistic model.

In recent years, model-free approaches have been described for the kinetic analysis of the cross-linking of resins such as epoxy [11–13], lignin-based [14], and phenolic resins [14,15] based on thermochemical data obtained from DSC. While such resins were successfully investigated by these methods, so far no attempts have been made to apply DSC–MFK to melamine–formaldehyde resins.

In the present contribution, a number of thermochemical methods are compared that allow the prediction of the curing behaviour of an MF resin based on a small set of designed experiments with dynamic differential scanning calorimetry (DSC). To study the effect of catalyst type and amount on the cross-linking kinetics of an industrial MF resin, four different commercial curing catalysts were mixed with MF resin in different proportions and the curing kinetics was quantitatively analyzed. By determining the curing enthalpy at different heating rates, the overall conversion dependent activation energy $E_a(\alpha)$ for the curing reaction was calculated and used to simulate the cross-linking kinetics of the resin mixtures at specified temperatures without any assumptions on the reaction mechanism. Theoretical curing isotherms were calculated from various mathematical approaches for model-free data analysis and the approach best suited for kinetic analysis of MF resin cross-linking was identified by comparison to the experimental data.

2. Experimental

2.1. Chemicals

Melamine formaldehyde pre-condensate was received as a gift from Impress Décor Austria GmbH (St. Donat, Austria). Four commercial catalyst preparations were also kindly donated by Impress Décor Austria GmbH.

2.2. Apparent curing time of catalysts

Four different industrial curing catalysts for MF resins were tested for their individual working range in catalyzing the cure of an industrial impregnation resin. Before use, the catalyst levels were adjusted with distilled water to the same acid equivalents upon titration with formaldehyde. Prior to DSC, the apparent curing time, $t_{c,a}$, of the resin/catalyst solutions was determined by preparing several catalyst/resin mixtures of different concentrations in test tubes and immersing the tubes in an oil bath at 100 °C under stirring until curing was completed. $t_{c,a}$ was measured as the time at which the resin turned completely white.

2.3. Differential scanning calorimetry

All thermograms were recorded using a differential scanning calorimeter 822e DSC by Mettler Toledo (Greifensee, Switzerland).

For the dynamic DSC experiments, the four normalized catalyst solutions were combined with industrial MF resin directly before recording the thermogram. Each resin sample contained 0.2, 0.4, or 0.6% (w/w) of one of the catalysts. To suppress vaporization of water and other volatiles during condensation, 2.0–3.5 mg of each resin sample was weighed into a high-pressure, gold-coated stainless

steel crucible (30 μL) which was sealed and subjected to a temperature gradient ranging from 25 to 250 °C with five heating rates (β = 2, 5, 10, 15 and 20 °C min^{-1}). The enthalpy changes were recorded and analyzed for the peak maximum, T_{peak}, and the enthalpy integral, H, using the STAR 8.10 software package (Mettler Toledo, Greifensee, Switzerland). All experiments were repeated twice.

For experimental verification of the kinetic models, validation experiments were performed using isothermal DSC. Here, 2.0–3.5 mg of each validation resin mixture was weighed into a high-pressure, gold-coated stainless steel crucible (30 μL) and thermograms were recorded at 80, 100 and 120 °C for 30 min. The validation samples were inserted into the oven which was preheated to the isothermal temperature. Thermograms were recorded after stabilization of the oven temperature which took approximately 1 min. As an alternative method, inserting the sample in the oven at room temperature and rapidly increasing the sample temperature to the isothermal level at a heating rate of 400 °C min^{-1} was tested, but not used for validation since overshooting of the temperature during the initial phase caused slightly stronger temperature exposure of the sample prior to the actual measurement and hence a larger experimental error. In all validation experiments, the enthalpy changes were recorded and analyzed for the peak maximum, T_{peak}, and the enthalpy integral, H.

2.4. Analysis of thermochemical data

From the temperature integral of the thermograms, both conversion, α, and the change of conversion with time, $\alpha(t) = d\alpha/dt$, were determined at a specific cure time (t). The $\alpha(t)$-value was determined from dynamic runs as the ratio between the heat released until a time t and the total heat of the reaction according to Eqs. (1) and (2):

$$\alpha(t) = \frac{H_{t_0 \ldots t}}{H_\infty} \tag{1}$$

$$\frac{d\alpha(t)}{dt} = \frac{H_t}{H_\infty}, \tag{2}$$

with t_0 = time of start of curing reaction and t_∞ = time of 100% cross-linking.

Integration of the enthalpy curve from t_0 to t yielded the degree of conversion $\alpha(t)$ for any time t between t_0 and t_∞ as the ratio $H_{t_0 \ldots t}/H_\infty$ where H_∞ is the integral of the enthalpy curve from t_0 to t_∞ and $H_{t_0 \ldots t}$ is the integral of the enthalpy curve from t_0 to t [14]. The differential $d\alpha/dt$ for each time t between t_0 and t_∞ was calculated as H_t/H_∞ where H_t is the current measured enthalpy at time t.

Kinetic analysis according to the model-free approaches by Friedman [16], Flynn–Wall–Ozawa [17,18] and Kissinger–Akahira–Sunose [19,20] was performed with the computer program Excel. For kinetic analysis according to the advanced Vyazovkin method [21], the STAR software package was used.

In the following section, the theory behind model-free kinetic approaches is shortly summarized. Starting with the basic rate equations, the different models used in this study are introduced and their main features are presented and compared.

3. Theory

3.1. Kinetic analysis—model dependent methods

All mathematical approaches to describe the curing kinetics of thermosets are based on the fundamental rate equation that relates the time dependent progression of conversion, $\alpha(t)$, at a constant temperature, T, to a function of the concentration of reactants, $f(\alpha)$, through a rate constant, k_T,

$$\left(\frac{d\alpha}{dt}\right)_T = k_T f(\alpha) \tag{3}$$

The temperature dependence of the rate constant follows the Arrhenius relationship:

$$k(T) = A \exp\left(-\frac{E_a}{RT}\right), \tag{4}$$

where A is the pre-exponential factor or Arrhenius frequency factor (s^{-1}), E_a is the activation energy (J mol^{-1}), R is the gas constant (8.314 J mol^{-1} K^{-1}), and T is the absolute temperature (K) of the sample.

To account for the temperature dependence of α, the kinetic model is combined with the Arrhenius equation and the reaction progress is expressed as

$$\frac{d\alpha}{dt} = A \exp\left(-\frac{E_a}{RT}\right) f(\alpha) \tag{5}$$

When the reaction mechanism is known, the reaction model $f(\alpha)$ can be derived and expressed as a function of the concentrations of the various components involved [22]. Depending on the type of chemical reaction, numerous $f(\alpha)$ have been described [23]. For example, if the thermosetting resin cure follows nth-order kinetics and the activation energy E_a is constant and independent of α, the rate of conversion is proportional to the reactant concentration and, according to Borchardt and Daniels [24], can be expressed as:

$$\frac{d\alpha}{dt} = A \exp\left(-\frac{E_a}{RT}\right) (1-\alpha)^n \tag{6}$$

Borchardt and Daniels [24] analyzed the nth-order curing reaction simply by taking the logarithm of Eq. (6) and plotting $\ln(d\alpha/dt)$ vs. T^{-1}. The activation energy E_a was determined as the slope by linear regression (=$-E_a/R$). However, to calculate the kinetic parameters multiple heating rates are required to keep the experimental error low [25].

However, the special case of E_a does not depend on α strictly applies only for very simple or elementary reactions. With more complicated reactions the activation energy for the overall process contains contributions of side or consecutive reactions. Thus, in most cases the assumption of E_a being independent of α is not valid and should better be expressed as $E_a(\alpha)$. Furthermore, with complex chemical reactions often the reaction model is not known or the mechanistic assumptions may be false. In such cases, approaches like the method suggested by Borchardt–Daniels fail. Instead the use of model-free kinetic (MFK) methods is preferable.

3.2. Kinetic analysis—model-free kinetics methods

With all MFK approaches the basic assumption is the isoconversional principle [26,27]. Taking logarithm of Eq. (5) and differentiating with respect to T^{-1} leads to

$$\ln\left(\frac{d\alpha}{dt}\right) = \ln(A) - \frac{E_a(\alpha)}{RT} + \ln f(\alpha) \tag{7}$$

$$d\ln\frac{(d\alpha/dt)}{dT^{-1}} = \frac{d\ln(A)}{dT^{-1}} - \frac{E_a(\alpha)}{R} + \frac{d\ln f(\alpha)}{dT^{-1}} \tag{8}$$

In the isoconversional assumption, the terms $d\ln(A)/dT^{-1}$ and $d\ln f(\alpha)/dT^{-1}$ are zero and the relation simplifies to

$$d\ln\frac{d\alpha/dt}{dT^{-1}} = -\frac{E_a(\alpha)}{R} \tag{9}$$

Since $d\ln f(\alpha)/dT^{-1} = 0$, no *a priori* knowledge on the reaction mechanism is required and errors due to wrong reaction model selection are avoided. The reaction rate $d\alpha/dt$ at a certain conversion α only depends on the temperature. Another important

feature is that with MFK methods E_a is determined in dependence of conversion as $E_a(\alpha)$. Several isoconversional methods have been developed to find the $E_a(\alpha)$ function. The methods can be classified in *differential methods* like the Friedman method (FR) [16] and *integral methods* like the Flynn–Wall–Ozawa method (FWO) [17,18], the Kissinger–Akahira–Sunose method (KAS) [19,20] or the Vyazovkin method [21]. The Vyazovkin method is known in its original (VO) and its advanced form (VA). The latter is obtained by mathematical modification of VO [21,28,29].

Like the Borchardt–Daniels (BD) method [24], the Friedman (FR) method is a differential method since they are both based on Eq. (5) with α as variable [16]. However, whereas the BD approach requires a reaction model $f(\alpha)$ and calculates only a constant activation energy E_a the FR method is not limited by these assumptions. By including the non-isothermal heating rate β (=dT/dt) in Eq. (5),

$$\frac{\beta\, d\alpha}{dT} = A \exp\left(\frac{-E_a(\alpha)}{RT}\right) f(\alpha) \tag{10}$$

and in its logarithmic form,

$$\ln\left(\frac{\beta\, d\alpha}{dT}\right) = \ln A + \ln f(\alpha) - \frac{E_a(\alpha)}{RT} \tag{11}$$

a linearized relationship is obtained from which $E_a(\alpha)$ can be determined by linear regression after plotting $\ln(\beta\, d\alpha/dT)$ vs. T^{-1} for different values of α. The terms $\ln(\beta\, d\alpha/dT)$ and T^{-1} at arbitrary values for α are obtained from the $\alpha(t)$ diagrams for each heating rate β.

Although being more widely applicable than model dependent approaches, the FR method suffers from some disadvantages as described by Vyazovkin [21] and Golikeri and Luss [30]. Since instantaneous rate values are employed, the method is numerically unstable [21] and the individual E_a obtained may differ largely from the apparent $E_a(\alpha)$ calculated by differential isoconversional methods [30]. To avoid these shortcomings, other methods are based on Eq. (5) in its integral form:

$$g(\alpha) = \int_0^{\alpha} \frac{d\alpha}{f(\alpha)} = A \int_0^{t} \exp\left(\frac{-E_a(\alpha)}{RT}\right)\, dt = AJ[E_a(\alpha), T] \tag{12}$$

where $g(\alpha)$ is the integral form of the reaction model $f(\alpha)$, and $T(t)$ is the heating program. For a linear heating rate $\beta = dT/dt$, $T(t)$ is linear and in Eq. (12), dt can be substituted by dT/β

$$g(\alpha) = \int_0^{\alpha} \frac{d\alpha}{f(\alpha)} = \frac{A}{\beta} \int_0^{T} \exp\left(\frac{-E_a(\alpha)}{RT}\right)\, dT = \frac{A}{\beta} I[E_a(\alpha), T] \tag{13}$$

Crucial with all integral methods is to solve the temperature integrals, I and J, respectively. Since they have no exact analytical solution [31], many authors have developed numerical approximations [28,32–36].

The FWO method [17,18] uses Doyle's approximation [32]:

$$\ln(I[E_a(\alpha), T]) = \ln \int_0^{T} \exp\left(\frac{-E_a(\alpha)}{RT}\right)\, dT = -5.331 - 1.052\frac{E_a(\alpha)}{RT} \tag{14}$$

and the integral form of Eq. (5) is expressed as

$$\ln(\beta) = A' - \frac{1.052 E_a(\alpha)}{RT} \tag{15}$$

with $A' = \ln(AE_a(\alpha)/R) - \ln g(\alpha) - 5.331$.

Again, the temperature integral approximation is substituted in Eq. (13) and the activation energy $E_a(\alpha)$ is determined by linear regression after plotting $\ln(\beta)$ vs. T^{-1}. Again, T^{-1} is obtained from the $\alpha(t)$-diagram for each heating rate β.

A similar approach based on the approximation of the temperature integral suggested by Coats and Redfern [33] was first suggested by Kissinger [19] and is known as the Kissinger–Akahira–Sunose (KAS) method [19,20]. According to KAS, the integral form of Eq. (5) is written as

$$\ln\left(\frac{\beta}{T^2}\right) = A' - \frac{E_a(\alpha)}{RT} \tag{16}$$

with

$$A' = \ln\left(\frac{AR}{E_a(\alpha)}\right) - \ln g(\alpha) \tag{17}$$

Again, E_a is calculated by linear regression after plotting $\ln(\beta/T^2)$ vs. T^{-1}. Although both the FWO and the KAS methods in many cases lead to much better results than earlier approaches, they are both limited by method selected for approximating the temperature integral. This may represent an illegitimate oversimplification and needs a correction especially for smaller values of $E_a(\alpha)/RT$ [37]. Table 1 summarizes the applied mathematical approaches for calculation of the activation energy and points out the coefficients used to determine E_a.

To avoid this dependence on the numerical approximation, Vyazovkin developed a completely different approach to solve the temperature integral [38]. He used the fact that for any heating rate β, the integral form $g(\alpha)$ is constant. Thus, with three heating rates β_1, β_2 and β_3, the integrals $g(\alpha)_{\beta_1} = g(\alpha)_{\beta_2} = g(\alpha)_{\beta_3}$ or

$$\frac{A}{\beta_1} I[E_a(\alpha), T]_1 = \frac{A}{\beta_2} I[E_a(\alpha), T]_2 = \frac{A}{\beta_3} I[E_a(\alpha), T]_3 \tag{18}$$

Consequently, A can be truncated and six equations can be formulated

$$\begin{aligned} \frac{J[E_a(\alpha), T]_1\beta_2}{J[E_a(\alpha), T]_2\beta_1} = 1 \text{ and } \frac{J[E_a(\alpha), T]_2\beta_1}{J[E_a(\alpha), T]_1\beta_2} = 1 \text{ and } \frac{J[E_a(\alpha), T]_1\beta_3}{J[E_a(\alpha), T]_3\beta_1} \\ = 1 \text{ and } \frac{J[E_a(\alpha), T]_3\beta_1}{J[E_a(\alpha), T]_1\beta_3} = 1 \text{ and } \frac{J[E_a(\alpha), T]_2\beta_3}{J[E_a(\alpha), T]_3\beta_2} \\ = 1 \text{ and } \frac{J[E_a(\alpha), T]_3\beta_2}{J[E_a(\alpha), T]_2\beta_3} = 1 \end{aligned} \tag{19}$$

which can be summarized as

$$\sum_{i=1}^{n}\sum_{j\neq 1}^{n} \frac{I[E_a(\alpha), T]_i\beta_j}{I[E_a(\alpha), T]_j\beta_i} = 6 \text{ for } n = 3 \tag{20}$$

With the VO method, $E_a(\alpha)$ is determined by iteration and minimizing Eq. (20). For example, in the case of an experiment with three heating rates the minimum ideally approaches six with deviations caused by an inherent experimental error. In contrast to FWO and KAS, the VO method enables free selection of both the temperature integral approximation as well as of the integration limits. Since FWO, KAS and VO all use the regular integration from 0 to T, single values for E_a are "averaged" over the region 0–α, and the function $E_a(\alpha)$ displays an undesired flattening [29]. To avoid this systematic error, Vyazovkin later replaced the regular integration by integration over small time segments [21]:

$$J[E_a(\alpha), T] = \int_{t_\alpha - \Delta\alpha}^{t_\alpha} \exp\left(-\frac{E_a(\alpha)}{RT}\right)\, dt \tag{21}$$

The value for $\Delta\alpha = 0.1$ was used for the calculations. It was based on nine equidistant intervals m and derived from the formula $\Delta\alpha = (m+1)^{-1}$. By choosing smaller intervals in $\Delta\alpha$, e.g. by choosing more equidistant intervals the error in estimating the activation energy would be further reduced by averaging the integral over smaller areas which is of advantage in reactions where strong variations of the activation energy are observed [21]. In the present case, the variations in $E_a(\alpha)$ were generally not very high and the choice of $\Delta\alpha$ was not critical.

Table 1
Derivation of the activation energy $E_a(\alpha)$ for the isoconversional (model-free) methods FR, FWO, KAS, VO, and VA, and the derivation of constant E_a and A from one model fitting approximation of Coats and Redfern (CR) to estimate A for an E_a.

Method	Function, one for each α	Approach	y	x	k	A'
FR	$\ln(\beta d\alpha/dT) = -E_a(\alpha)/RT + (\ln A + \ln f(\alpha))$	$y = kx + A'$[a]	$\ln(\beta\, d\alpha/dT)$	$1/T$	$-E_a(\alpha)/R$	$\ln A + \ln f(\alpha)$
FWO	$\ln(\beta) = -1.052E_a(\alpha)/RT + (\ln(AE_a/R) - \ln g(\alpha) - 5.331)$	$y = kx + A'$[a]	$\ln(\beta)$	$1/T$	$-1.052E_a(\alpha)/R$	$\ln(AE_a(\alpha)/R) - \ln g(\alpha) - 5.331$
KAS	$\ln(\beta/T^2) = -E_a(\alpha)/RT + (\ln(AR/E_a(\alpha)) - \ln g(\alpha))$	$y = kx + A'$[a]	$\ln(\beta/T^2)$	$1/T$	$-E_a(\alpha)/R$	$\ln(AR/E_a(\alpha)) - \ln g(\alpha)$
VO	$\sum_{i=1}^{n}\sum_{j\neq 1}^{n} \frac{I[E_a(\alpha),T]_i\beta_j}{I[E_a(\alpha),T]_j\beta_i} = \min$ with $I[E_a(\alpha),T] = \int_0^T \exp\left(\frac{-E_a(\alpha)}{RT}\right) dT$	$E_a(\alpha) = \min$[b]	–	–	–	–
VA	$\sum_{i=1}^{n}\sum_{j\neq 1}^{n} \frac{J[E_a(\alpha),T]_i}{J[E_a(\alpha),T]_j} = \min$ with $J[E_a(\alpha),T] = \int_{t_\alpha-\Delta\alpha}^{t_\alpha} \exp\left(\frac{-E_a(\alpha)}{RT}\right) dt$	$E_a(\alpha) = \min$[b]	–	–	–	–
CR	$\ln(g(\alpha)/T^2) = -E_a/RT + \ln(AR/\beta E_a)$	$y = kx + A'$[c]	$\ln(g(\alpha)/T^2)$	$1/T$	$-E_a/R$	$\ln(AR/\beta E_a)$

[a] Calculation of $E_a(\alpha)$ is based on the linear regression of y and x to obtain slope k including $E_a(\alpha)$. Calculation of A from complex A' is not possible.
[b] Calculation of $E_a(\alpha)$ is based on the numerical minimization of function to get current the value of $E_a(\alpha)$ at the found minimum (no calculation of A is performed).
[c] Calculation of E_a is based on the linear regression of y and x to get slope k including constant E_a and intercept A' including constant A. From each heating rate β one curve $\alpha(t)$ is obtained. In this case, a reaction model is required.

The reaction time t_α, when the curing has progressed to a degree of conversion α is calculated by

$$t_\alpha = \frac{\int_0^T \exp(-E_a(\alpha)/RT)\ dT}{\beta \exp(-E_a(\alpha)/RT_0)} \quad (22)$$

Using Eq. (22), the $\alpha(t)$-diagrams for an arbitrary isothermal temperature T_0 can be calculated [39].

4. Results and discussion

4.1. Thermochemical analysis

The curing kinetics of an industrial melamine–formaldehyde resin containing four different types of commercial curing catalysts at three concentration levels was studied using dynamic DSC. The conversion–time diagrams $\alpha(t)$ were determined from measurements at five heating rates, β = 2, 5, 10, 15 and 20 °C min^{-1} and used as the raw data for isoconversional kinetic analysis. Fig. 2 shows typical thermograms for the curing of a mixture of MF resin with 0.4% catalyst A with a linear increase in temperature at the various heating rates β.

The initial increase in exothermal enthalpy at time t_0 indicates the start of the resin cross-linking and corresponds to a conversion of α = 0. After reaching a maximum, the enthalpy decreases until curing is completed at time t_∞ at a conversion of α = 1.

Table 2 summarizes the thermochemical parameters obtained from the DSC experiments for the various resin/catalyst mixtures at a heating rate of β = 10 °C min^{-1}. In addition to DSC analysis, curing experiments with the catalyst were performed in test tubes according to the standard procedure used in the industry and the apparent curing times $t_{c,a}$ are also given in Table 2. For all individual systems, $t_{c,a}$ decreased as the catalyst concentration increased. Addition of higher amounts of catalyst led to a lower initial pH in the impregnation solution. $t_{c,a}$ as well as T_p and T_o decreased with a decrease in initial pH of the resin formulation. The total normalized enthalpies were all of the same order of magnitude around 60 J g^{-1} and independent of the amount of catalyst used. With increasing levels of catalyst, however, the T_p- and T_o-values significantly shifted to lower temperatures. The results shown in Table 2 illustrate that the rate of curing is accelerated with an increase in catalyst concentration. Although the $t_{c,a}$ already gives a preliminary indication of the reactivity of the used catalyst system, no quantitative prediction on the required pressing conditions (reaction time and temperature, conversion) can be deduced from these data. For this a more detailed analysis of the DSC data is required.

From the exothermic DSC data, the temperature dependent degree of conversion $\alpha(t)$ was derived. In Fig. 3, the degree of conversion $\alpha(t)$ is plotted against the temperature for the five heating rates β. The data from the conversion curves were used as basis for the kinetic analysis with different isoconversional methods.

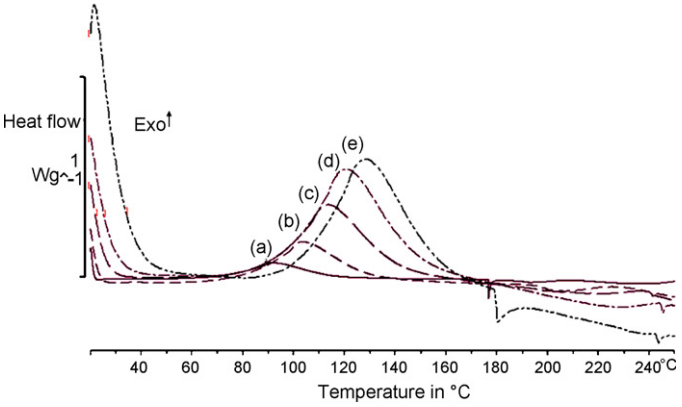

Fig. 2. DSC thermograms of MF resin containing 0.4% of resin curing catalyst A at different heating rates. (a) 2 °C min^{-1}, (b) 5 °C min^{-1}, (c) 10 °C min^{-1}, (d) 15 °C min^{-1}, and (e) 20 °C min^{-1}.

Table 2
Average enthalpy integral (H), peak temperature (T_p) and peak onset temperature (T_o) obtained from the DSC thermograph of MF resin containing different concentrations (C) of different curing catalysts. The pH and apparent curing time ($t_{c,a}$) of the resin mixtures is also given.

Catalyst	C (%, w/w)	H[a] (J g^{-1})	T_p[a] (°C)	T_o[a] (°C)	pH	$t_{c,a}$ (min)
A	0.2	57.18	120	105	7.72	4.54
	0.4	58.24	113	98	7.44	3.07
	0.6	59.33	110	95	7.20	2.21
B	0.2	64.87	122	105	7.66	4.52
	0.4	60.50	112	97	7.42	2.41
	0.6	63.67	108	92	7.24	2.00
C	0.3	60.22	123	106	7.78	5.07
	0.5	58.01	117	100	7.61	3.27
	0.7	62.03	115	98	7.51	2.41
D	0.3	62.38	126	108	7.69	5.41
	0.5	59.21	117	100	7.47	3.18
	0.7	44.63	114	97	7.33	2.27

[a] Measured at a heating rate β of 10 °C min^{-1}.

Table 3
Kinetic parameters $E_a(\alpha)$ in kJ mol^{-1} and A' (=ln(($A \times E_a(\alpha)$)/($R \times g(\alpha)$) − 5.331)) for catalysts A and C at 0.4 and at 0.6% derived from Flynn–Wall–Ozawa (FWO) isoconversional method.

α (%)	A, 0.4%			A, 0.6%			C, 0.4%			C, 0.6%		
	A'	E_a (kJ mol^{-1})	R^2	A'	E_a (kJ mol^{-1})	R^2	A'	E_a (kJ mol^{-1})	R^2	A'	E_a (kJ mol^{-1})	R^2
10	29.66	80.13	0.997	28.43	75.75	0.993	25.81	68.68	0.985	27.27	71.74	0.991
20	29.27	80.38	0.998	28.05	76.03	0.995	25.71	69.65	0.988	26.76	71.6/	0.992
30	29.03	80.61	0.998	27.76	76.08	0.995	25.61	70.19	0.988	26.47	71.72	0.993
40	28.81	80.65	0.998	27.49	75.93	0.995	25.40	70.21	0.988	26.17	71.49	0.993
50	28.53	80.43	0.998	27.18	75.60	0.995	25.18	70.10	0.987	25.91	71.29	0.993
60	28.36	80.53	0.998	26.97	75.54	0.995	25.01	70.11	0.985	25.75	71.38	0.993
70	28.24	80.84	0.997	26.76	75.55	0.994	24.81	70.20	0.983	25.63	71.62	0.993
80	28.15	81.35	0.997	26.56	75.68	0.994	24.68	70.36	0.980	25.54	72.07	0.993
90	28.03	82.11	0.996	26.30	75.90	0.993	24.50	70.76	0.976	25.53	73.08	0.993
98	28.20	84.58	0.987	26.27	77.54	0.987	24.51	72.48	0.963	26.14	77.02	0.993

Table 4
Kinetic parameters $E_a(\alpha)$ in kJ mol^{-1} and A' (=ln($A \times f(\alpha)$)) for catalysts A and C at 0.4 and at 0.6% derived from Friedman (FR) isoconversional method.

α (%)	A, 0.4%			A, 0.6%			C, 0.4%			C, 0.6%		
	A'	E_a (kJ mol^{-1})	R^2	A'	E_a (kJ mol^{-1})	R^2	A'	E_a (kJ mol^{-1})	R^2	A'	E_a (kJ mol^{-1})	R^2
10	23.47	79.00	0.998	22.19	74.36	0.998	20.13	68.70	0.986	20.53	68.88	0.990
20	23.46	78.72	0.998	22.18	74.05	0.998	20.72	68.90	0.984	20.77	69.31	0.992
30	24.01	80.40	0.998	22.24	74.18	0.998	20.31	70.01	0.983	21.02	69.95	0.994
40	22.75	76.40	0.997	21.33	71.26	0.997	19.76	66.86	0.978	20.15	67.13	0.992
50	23.18	78.27	0.996	21.44	72.05	0.996	19.89	67.63	0.972	20.49	68.62	0.991
60	23.25	79.28	0.996	21.50	72.96	0.996	19.92	68.36	0.969	20.65	69.77	0.991
70	23.35	80.69	0.994	21.42	73.71	0.994	19.66	68.46	0.964	20.66	70.80	0.991
80	23.09	81.45	0.992	21.06	74.01	0.992	19.40	69.06	0.961	20.50	71.80	0.992
90	22.50	82.20	0.986	20.42	74.44	0.986	19.04	70.46	0.948	20.52	74.68	0.991
98	20.15	78.38	0.984	18.21	70.90	0.984	16.48	65.65	0.952	18.02	70.16	0.990

4.2. Calculation of activation energy $E_a(\alpha)$

In the first step, a suitable mathematical approach for the model-free kinetic analysis of the curing of the different MF/catalyst systems was selected based on the comparison of four isoconversional methods. The isoconversional method that fitted best the experimental data obtained from isothermal measurements was further used to discuss some effects of the different catalyst types and amounts (Section 4.3). From Fig. 3, for each β, corresponding pairs of values for T and α were extracted to plot ln(β), ln($\beta\, d\alpha/dT$), or ln(β/T^2) vs. T^{-1} to determine the activation energy $E_a(\alpha)$ and the pre-exponential factor A' using the FWO, FR and KAS isoconversional methods (see Table 1). E_a, A', and the corresponding correlation coefficient R^2 that were calculated with the FWO, FR, and KAS methods are given in Tables 3–5. In Table 6, the activation energy $E_a(\alpha)$ calculated with the advanced form of the Vyazovkin model is depicted for different degrees of conversion α.

Although kinetic analysis was performed with the total set of data, only four selected resin/catalyst mixtures are shown for illustration in the tables. The selected runs were at low and high concentration levels of catalyst A and C since these two catalyst systems showed the largest differences in curing behaviour. Fig. 4 illustrates the conversion-dependent activation energy, $E_a(\alpha)$, for the low level of catalyst A to highlight the differences between the models. For better visibility, representative error bars are only indi-

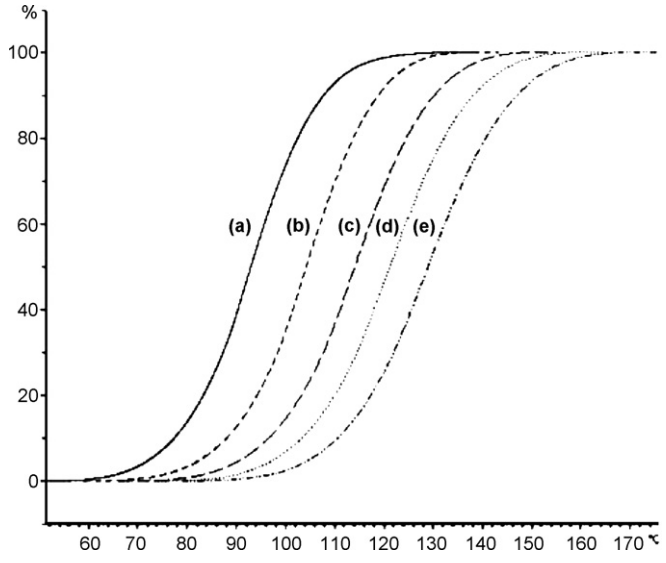

Fig. 3. Temperature dependence of the degree of conversion $\alpha(t)$ of an MF resin containing 0.4% curing catalyst A at different heating rates during recording of the thermogram (T—temperature in DSC vessel). (a) 2 °C min^{-1}, (b) 5 °C min^{-1}, (c) 10 °C min^{-1}, (d) 15 °C min^{-1}, and (e) 20 °C min^{-1}.

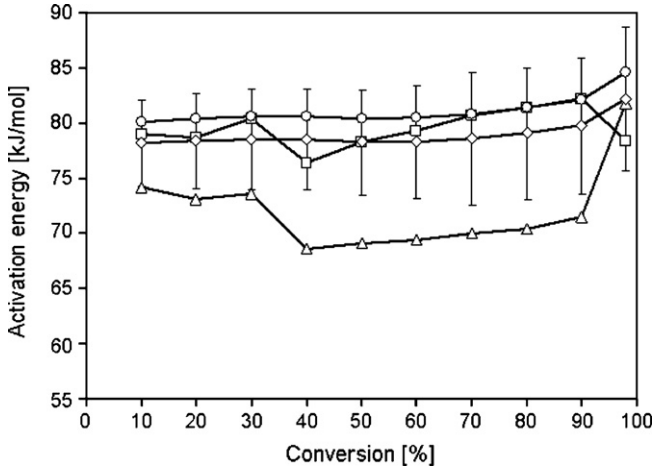

Fig. 4. Activation energy E_a in kJ mol^{-1} for catalyst A at 0.4%, estimated by four different isoconversional methods: Friedman (FR, □), Kissinger–Akahira–Sunose (KAS, ◇), advanced Vyazovkin (VA, △); Flynn–Wall–Ozawa (FWO, ○).

Table 5
Kinetic parameters $E_a(\alpha)$ in kJ mol^{-1} and A' (=ln(($A \times R$)/($E_a(\alpha) \times g(\alpha)$))) for catalysts A and C at 0.4 and at 0.6% derived from Kissinger–Akahira–Sunose (KAS) isoconversional method.

α (%)	A, 0.4%			A, 0.6%			C, 0.4%			C, 0.6%		
	A'	E_a (kJ mol^{-1})	R^2	A'	E_a (kJ mol^{-1})	R^2	A'	E_a (kJ mol^{-1})	R^2	A'	E_a (kJ mol^{-1})	R^2
10	15.86	78.22	0.996	14.65	73.67	0.992	12.02	66.20	0.982	13.51	69.53	0.989
20	15.43	78.38	0.997	14.24	73.86	0.993	11.88	67.11	0.985	12.96	69.33	0.990
30	15.17	78.55	0.997	13.92	73.84	0.994	11.75	67.61	0.986	12.65	69.31	0.991
40	14.93	78.53	0.997	13.63	73.63	0.994	11.53	67.58	0.985	12.33	69.01	0.992
50	14.64	78.26	0.997	13.31	73.23	0.994	11.30	67.41	0.984	12.06	68.76	0.992
60	14.46	78.31	0.997	13.08	73.12	0.994	11.11	67.38	0.982	11.88	68.80	0.991
70	14.32	78.58	0.997	12.83	73.08	0.993	10.93	67.41	0.980	11.74	69.00	0.991
80	14.20	79.06	0.996	12.63	73.15	0.992	10.74	67.52	0.976	11.63	69.41	0.991
90	14.06	79.77	0.995	12.31	73.28	0.991	10.54	67.85	0.971	11.59	70.38	0.992
98	14.18	82.21	0.984	12.27	74.86	0.985	10.50	69.49	0.955	12.15	74.36	0.991

cated for the dataset calculated with the KAS method to give an indication of the overall error.

Considering the error introduced by the calculation method and the experiment [25], with all methods practically the same constant E_a values was obtained which depended only slightly on α which is visible in a small increase toward the end of the reaction. Only with FR, $E_a(\alpha)$ finally decreased again significantly when curing was nearly completed. With FWO, $E_a(\alpha)$ increased only slightly until a conversion of $\alpha > 80\%$ was reached and increased very strongly with $\alpha > 90\%$. With KAS, generally slightly lower values for $E_a(\alpha)$ were obtained than with FWO. Again, $E_a(\alpha)$ slightly increased at $\alpha < 90\%$ and a steeper increase was obtained with $\alpha > 90\%$. With all methods, a slight decrease in $E_a(\alpha)$ was calculated around $\alpha \sim 40\%$, FR and VA leading to a more significant decrease in $E_a(\alpha)$ between 30 and 50% conversion than the other methods. In most cases, the correlation coefficients (R^2) were between 0.98 and 1.00. Although experimental error masks the effect, the kink in the course of $E_a(\alpha)$ corresponds to the observation that resins cured in test tubes started to form agglomerates when they had reached a theoretical conversion of ca. 40% which caused turbidity to the dispersion due to the lower water tolerance of the curing resin. Hence the characteristic shape of the activation energy curve could possibly be attributed to a phase transition that takes place when insoluble gels are formed and the minimum in $E_a(\alpha)$ could mark the transition to solidification of the resin.

4.3. Calculation of $\alpha(t)$ and MFK evaluation

The activation energy was used to calculate theoretical isothermal profiles of the degree of conversion, $\alpha(t)$, during the curing. These isotherms were compared to experimental isothermal curing profiles obtained from isothermal DSC measurements at various temperatures. The models were evaluated for best fit with the experimental data. In Fig. 5a–c, plots of $\alpha(t)$ calculated from the various models vs. reaction time t for three temperatures, 80 °C (Fig. 5a), 100 °C (Fig. 5b) and 120 °C (Fig. 5c) are depicted. The experimental curves are given for comparison. No mathematical method was able to predict the experimental data perfectly. With $\alpha(t) \leq 40\%$ the reaction profiles appeared very similar with all four models and all mathematical approaches fitted the experimental data quite well. With higher degrees of conversion the models deviated more significantly, the FR method giving the worst fit. The FR isoconversional method is different from the KAS and the FWO methods. While in KAS and FWO the conversion is directly related to T^{-1}, in FR for a given temperature the reaction rates ($r = da/dt$) at different degrees of cross-linking are obtained from dynamic DSC measurements. The model suitability varied with the temperature chosen for the isothermal runs. The best agreement of the calculated values with the experimental data was obtained with the run at 80 °C. While with 100 °C, the FWO method fitted the experimental data best, with the 120 °C the KAS and VA methods approximated the real data better and equally well. The FR method was in both cases the worst approximation. For all three temperatures the VA method was reasonably close to the experimental curve. Thus, the VA approach was assumed to be the most robust method with respect to temperature and was chosen to more closely investigate the influence of variations in curing catalyst type and amount at another temperature.

Although it is possible to determine kinetic parameters from isothermal DSC data this approach is not preferable for MF resins since reaction rates and enthalpy changes during MF cure are rather low and difficult to analyze accurately [40]. For the exact determination of the curing behaviour the use of pressurized crucibles made of stainless steel is required to suppress interfering signals from water and/or solvent evaporation. In such pressurized vessels the suboptimal thermal conductivity leads to a reduced sensitivity of the measurement. This is more of a problem with isothermal than with dynamic measurements, hence sensitivity with dynamic DSC is much better.

Moreover, with isothermal DSC measurements, the time dependence of α is determined directly for a defined temperature and hence is valid only for this chosen temperature. Thus, to determine the temperature dependence of α, numerous isothermal experiments at different temperatures are required. With dynamic experiments, isotherms are not determined directly. Kinetic analysis is based on dynamic measurements at different heating rates which allow the calculation of α as a function of temperature, $\alpha(T)$, based on only a few, typically three or five experiments [41].

The curing of MF has earlier been investigated on the basis of dynamic DSC measurements [40]. To analyze their thermograms, the authors used the ASTM E 698 method [42], which is basically founded on the Borchardt–Daniels approach described earlier (see Section 3, [24]). Based on an arbitrarily selected reaction model the corresponding activation energy and pre-exponential factor were determined, that were assumed to describe the MF system ade-

Table 6
Kinetic parameter $E_a(\alpha)$ in kJ mol^{-1} for catalysts A and C at 0.4 and at 0.6% derived from the advanced Vyazovkin (VA) isoconversional method.

α (%)	$E_a(\alpha)$ (kJ mol^{-1})			
	A		C	
	0.4%	0.6%	0.4%	0.6%
10	74.19	73.94	68.18	68.69
20	73.1	73.03	67.89	68.3
30	73.56	73.05	68.7	68.73
40	68.61	69.05	64.95	65.21
50	69.06	69.76	65.43	66.46
60	69.43	70.34	65.75	67.32
70	69.99	71.1	66.29	68.39
80	70.38	71.93	67.24	69.77
90	71.46	73.18	69.27	73.59
98	81.35	81.86	75.18	84.48

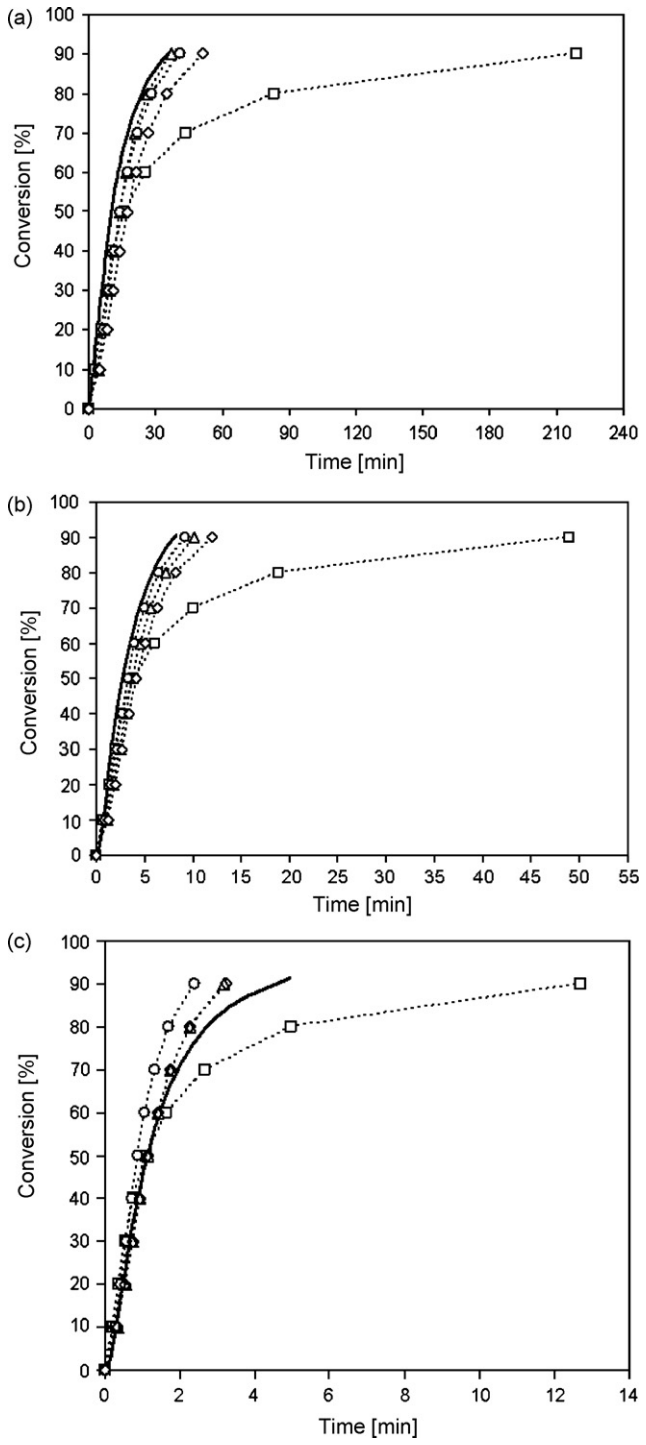

Fig. 5. (a) Conversion α in % over time for catalyst A at 0.4% and isothermal at 80 °C. Comparison of the isothermal experiment (—) with curves calculated with four different isoconversional methods: Friedman (FR, □), Kissinger–Akahira–Sunose (KAS, ◊), advanced Vyazovkin (VA, △); Flynn–Wall–Ozawa (FWO, ○). (b) Conversion α in % over time for catalyst A at 0.4% and isothermal at 100 °C. Comparison of the isothermal experiment (—) with curves calculated with four different isoconversional methods: Friedman (FR, □), Kissinger–Akahira–Sunose (KAS, ◊), advanced Vyazovkin (VA, △); Flynn–Wall–Ozawa (FWO, ○). (c) Conversion α in % over time for catalyst A at 0.4% and isothermal at 120 °C. Comparison of the isothermal experiment (—) with curves calculated with four different isoconversional methods: Friedman (FR, □), Kissinger–Akahira–Sunose (KAS, ◊), advanced Vyazovkin (VA, △); Flynn–Wall–Ozawa (FWO, ○).

quately throughout the curing reaction. The authors found that the assumed first order reaction kinetic model was not valid and thus they modified the reaction model underlying the ASTM E 698 algorithm until the calculated parameters fitted the experimental results satisfactorily [42]. Since with this approach for each different MF resin mixture a different setting in model equations is required, the method cannot be regarded as generally applicable and is thus of only limited use. Another shortcoming of the recent approach is the assumption of constant E_a. In the present study it was illustrated by any of the tested isoconversional approaches that E_a slightly changes during the curing reaction and that thus MF resin curing must be regarded as a "multi-step" process [11]. In such a multi-step process the concept of constant E_a does not lead to accurate predictive models [23]. Instead, isoconversional kinetics is preferable.

Alonso et al. [14] have verified the validity of the isoconversional principal for two types of formaldehyde based resins, a lignin–formaldehyde and phenol–formaldehyde resin, by measuring the gel-time at different temperatures. They found that although the degree of conversion α was different for the two resins, it was not dependent on the curing temperature and hence the isoconversional principle was valid. Since aminoplastic resins follow an analogous addition–condensation mechanism like phenolic resins during cross-linking, the isoconversional principle was assumed to be valid for the melamine–formaldehyde resin studied in the present study as well.

Besides performing isothermal experiments to validate the modelling power of the isoconversional kinetic approaches, in a related study the thermochemical parameters were related to the technological properties of products manufactured therefrom [43]. For this, the conversion-dependent activation energy for the MF curing as calculated by the VA method was used to calculate isotherms which in turn were employed in combination with a technological data set to describe the influence of some processing parameters on the surface properties of the laminated boards. By using MFK derived isotherms as the basis and conversion as a variable in a response surface model, it was possible to predict the gloss, the cleanability and to a lesser degree the chemical resistance of laminate surfaces. The results are described in detail in [43] and illustrate the usefulness of isoconversional analysis in solving engineering problems.

4.4. Comparison of different catalysts

Fig. 6 shows the conversion dependent activation energy $E_a(\alpha)$ for different curing catalysts and different catalyst levels as calculated with the advanced Vyazovkin approach. In Fig. 7, the corresponding isothermal time profiles of α are shown for 150 °C.

Although the two different catalysts yield different values for E_a, the overall shape of $E_a(\alpha)$ is the same and is similar to the shape obtained for MF curing without any addition of catalyst. Up to conversions of 40%, the catalyst amounts seem to have no impact on the activation energy. $E_a(\alpha)$ for the high and the low catalyst levels are indistinguishable from each other. Interestingly, in both cases with the higher catalyst levels larger values for $E_a(\alpha)$ are obtained. This illustrates that the calculated values for $E_a(\alpha)$ may not be the only relevant entities to explain the effect of catalyst concentration. An increase in catalyst concentration may have no effect on E_a because saturation may have been reached at 0.4%. Also, an increase in catalyst concentration not necessarily needs to lead to a decrease of activation energy when the catalyst acts by increasing the efficiency of molecular interactions which would be visible in A or $f(\alpha)$. Above all, the differences in the calculated values for $E_a(\alpha)$ are statistically of little significance since it is known that the confidence interval for $E_a(\alpha)$ calculated with the VA method is 10–20% [44]. This ren-

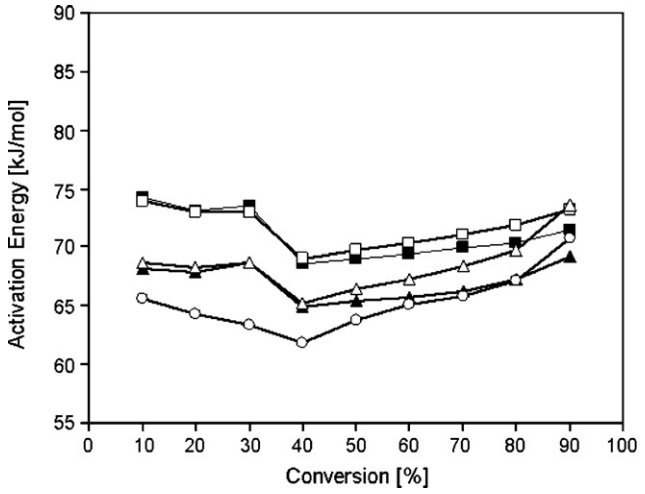

Fig. 6. The activation energy $E_a(\alpha)$ as calculated with the advanced Vyazovkin method (VA) for MF resin samples containing catalyst A at 0.4 wt% (■) and at 0.6% (□) and containing catalyst C at 0.4 wt% (▲), at 0.6% (△), and without catalyst (○).

ders mechanistic discussions difficult in the present case although $E_a(\alpha)$ is adequate for the practical purpose of predicting isothermal kinetics (see Fig. 7, [14,23,45,46]).

From the DSC–MFK analysis, the time required for 90% conversion at a certain temperature can be calculated for each of the resin/catalyst mixtures. In Table 7, these values are summarized for two catalyst systems for a temperature interval from 40 to 180 °C. Although in the present study, the course of the isotherms is only shown up to a conversion of 90%, this does not mean that the models would not be applicable to produce values also for a higher degree of conversion. However, with values close to 100% all models significantly start to be more erroneous due to effects during curing such as diffusional limitation. As for a specific technological application such as the impregnation of decorative papers and subsequent laminate formation, curing degrees of higher than 90% are typically not reached by the resin in the impregnated paper prior to the pressing since the papers must remain self-gluing. Even upon pressing to the laminate, the resins are practically never fully cured during the lamination in the hot press in the thermochemical sense which can be seen in the variations in dimensional stability behaviour of the coated particleboards caused by post-curing induced shrinking processes [5].

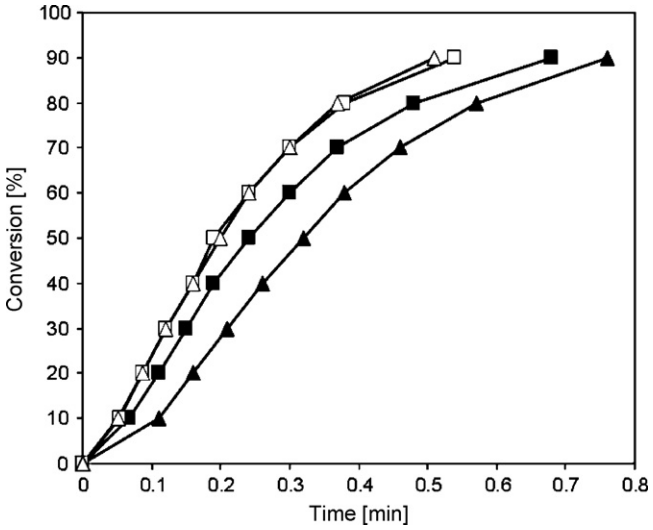

Fig. 7. The conversion α (%) vs. time, t (min), as calculated with the advanced Vyazovkin method (VA) for MF resin samples containing catalyst A at 0.4 wt% (■) and at 0.6% (□) and containing catalyst C at 0.4 wt% (▲) and at 0.6% (△) for 150 °C.

Table 7
Time required for 90% conversion for catalysts A and C at 0.4 and at 0.6% derived from the advanced Vyazovkin (VA) isoconversional method at various temperatures.

T (°C)	t_{90}[a] (min)			
	A		C	
	0.4%	0.6%	0.4%	0.6%
40	820.69	693.40	592.29	511.94
50	352.16	295.11	267.04	224.58
60	159.05	132.24	126.37	103.58
70	75.27	62.11	62.50	50.00
80	37.17	30.45	32.19	25.16
90	19.09	15.53	17.21	13.16
100	10.16	8.22	9.52	7.13
110	5.59	4.49	5.43	3.99
120	3.17	2.53	3.19	2.30
130	1.85	1.47	1.93	1.36
140	1.11	0.88	1.19	0.83
150	0.68	0.54	0.76	0.51
160	0.43	0.33	0.49	0.33
170	0.27	0.21	0.32	0.21
180	0.18	0.14	0.22	0.14

[a] t_{90}: time required for 90% conversion at a specified temperature.

From Table 7 it is seen that the two different catalyst systems display different temperature response in their catalytic behaviour. While at high catalyst levels, catalyst C always causes faster curing than catalyst A, at low catalyst levels this is only true for temperatures up to 110 °C. At higher temperatures, catalyst A is more effective than C. This technologically important behaviour can be attributed to the different de-blocking characteristics of different MF catalysts, meaning that the catalytically active acidic component in the catalyst is liberated upon temperature dependent dissociation and evaporation of a blocking component. Hence, by applying DSC–MFK it is possible to detect and characterize the de-blocking behaviour of different catalysts for MF curing.

5. Conclusion

The curing of an MF impregnation resin containing different types and amounts of curing catalysts was studied by dynamic DSC. Based on the experimental data, conversion $\alpha(t)$ as a function of time and the conversion dependent activation energy $E_a(\alpha)$ were calculated using the mathematical approaches for kinetic analysis by Friedman, Flynn–Wall–Ozawa, Kissinger–Akahira–Sunose and Vyazovkin. By comparison with isothermal DSC experiments at selected temperatures, the different approaches were evaluated for their accuracy in predicting the curing behaviour in a temperature range relevant for the thermofusing step in laminates production. It was found that the advanced Vyazovkin method was superior to the other methods. The presented results illustrate that model-free isoconversional methods for kinetic analysis of thermochemical data can be applied to the investigation and optimization of melamine–formaldehyde resins.

References

[1] H. Kamola, Focus on melamine, in: Proc Int. Surf. Conf., Amsterdam, Netherlands, 28–29 March, 2007, pp. 89–93.
[2] A. Pizzi, Advanced Wood Adhesives Technology, Marcel Dekker Inc., New York, USA, 1994.
[3] C. O'Carroll, European market update, in: Proc. Europ. Lamin. Conf., Berlin, Germany, 19–22 April 2004, 2004, P1, 1–12.
[4] A.T. Mercer, A. Pizzi, A 13C-NMR analysis method for MF and MUF resin strength and formaldehyde emission from wood particleboard. II. MF resins, J. Appl. Polym. Sci. 61 (10) (1996) 1697–1702.
[5] A. Kandelbauer, A. Teischinger, On the warping behaviour of particleboards coated with melamine formaldehyde resin impregnated papers, Eur. J. Wood Prod. (2009), doi:10.1007/s00107-009-0327-z (published online April 10, 2009).

[6] P. Petek, A. Böttcher, A. Kandelbauer, Experimental design methods for the optimization of impregnation resins, in: Proc. Europ. Lamin. Conf., Prague, Czech Rep., 4–6 April 2006, 2006, P7, 1–7.
[7] J. Mijatowic, W.H. Binder, F. Kubel, W. Kantner, Studies on the stability of MF resin solutions: investigations on network formation, Macromol. Symp. 181 (2002) 373–382.
[8] A. Kandelbauer, Online control of melamine formaldehyde resin by mid infrared ATR spectroscopy and multivariate curve resolution, in: 1st Int. CAMO User Meeting on Multivar. Data Anal., Frankfurt, Germany, 28–29 April 2006, 2006.
[9] A. Kandelbauer, A. Despres, A. Pizzi, I. Taudes, Testing by Fourier Transform infrared species variation during melamine–urea–formaldehyde resin preparation, J. Appl. Polym. Sci. 106 (2007) 2192–2197.
[10] A. Despres, A. Pizzi, H. Pasch, A. Kandelbauer, Comparative 13C-NMR and matrix-assisted laser desorption/ionization time-of-flight analyses of species variation and structure maintenance during melamine–urea–formaldehyde resin preparation, J. Appl. Polym. Sci. 106 (2007) 1106–1128.
[11] S. Vyazovkin, N. Sbirrazzuoli, Mechanism and kinetics of epoxy-amine cure studied by differential scanning calorimetry, Macromolecules 29 (1996) 1867–1873.
[12] N. Sbirrazzuoli, S. Vyazovkin, Learning about epoxy cure mechanisms from isoconversional analysis of DSC data, Thermochim. Acta 388 (2002) 289–298.
[13] W. Liu, Q. Qiu, J. Wang, Z. Huo, H. Sun, Curing kinetics and properties of epoxy resin–fluorenyl diamine systems, Polymer 49 (20) (2008) 4399–4405.
[14] M.V. Alonso, M. Oliet, J. García, F. Rogríguez, J. Echeverría, Gelation and isoconversional kinetic analysis of lignin–phenol–formaldehyde resol resins cure, Chem. Eng. J. 122 (2006) 159–166.
[15] J. Wang, M.-P.G. Laborie, M.P. Wolcott, Comparison of model-free kinetic methods for modelling the cure kinetics of commercial phenol formaldehyde resins, Thermochim. Acta 439 (2005) 68–73.
[16] H.L. Friedman, Kinetics of thermal degradation of char-forming plastics from thermogravimetry, application to a phenolic plastic, J. Polym. Sci. Part C 6 (1965) 183–195.
[17] J.H. Flynn, L.A. Wall, General treatment of the thermogravimetry of polymers, J. Res. Natl. Bur. Stand. A: Phys. Chem. 70 (6) (1966) 487–523.
[18] T. Ozawa, A new method of analyzing thermogravimetric data, Bull. Chem. Soc. Jpn. 38 (1) (1965) 1881–1886.
[19] H.E. Kissinger, Reaction kinetics in differential thermal analysis, Anal. Chem. 29 (11) (1957) 1702–1706.
[20] T. Akahira, T. Sunose, Res. Rep. Chiba Inst. Technol. (Sci. Technol.) 16 (1971) 22.
[21] S. Vyazovkin, Modification of the integral isoconversional method to account for variation in the activation energy, J. Comput. Chem. 22 (2) (2001) 178–183.
[22] M.E. Brown, D. Dollimore, A.K. Galwey, Reactions in the Solid State, Comprehensive Chemical Kinetics, vol. 22, Elsevier, Amsterdam, 1980.
[23] S. Vyazovkin, C.A. Wight, Model-free and model-fitting approaches to kinetic analysis of isothermal and nonisothermal data, Thermochim. Acta 340–341 (1999) 53–68.
[24] H.J. Borchardt, F.J. Daniels, The application of differential thermal analysis to the study of reaction kinetics, J. Am. Chem. Soc. 79 (1) (1957) 41–46.
[25] S. Vyazovkin, Two types of uncertainty in the values of activation energy, J. Therm. Anal. Calorim. 64 (2001) 829–835.
[26] S. Vyazovkin, Isoconversional kinetics, in: M.E. Brown, P.K. Gallagher (Eds.), The Handbook of Thermal Analysis & Calorimetry, vol. 5: Recent Advances, Techniques and Applications, Elsevier, 2008, pp. 503–538 (Ch. 13).
[27] S. Vyazovkin, N. Sbirrazzuoli, Isoconversional kinetic analysis of thermally stimulated processes in polymers, Macromol. Rapid Commun. 27 (18) (2006) 1515–1532.
[28] P. Budrugeac, E. Segal, Some methodological problems concerning nonisothermal kinetic analysis of heterogeneous solid-gas reactions, Int. J. Chem. Kinet. 33 (10) (2001) 564–573.
[29] S. Vyazovkin, Some confusion concerning integral isoconversional methods that may result from the paper by Budrugeac and Segal Some Methodological Problems Concerning Nonisothermal Kinetic Analysis of Heterogeneous Solid-Gas Reactions, Int. J. Chem. Kinet. 34 (7) (2002) 418–420.
[30] S.V. Golikeri, D. Luss, Analysis of activation energy of grouped parallel reactions, J. Am. Chem. Eng. 18 (2) (1972) 277–282.
[31] I.N. Bronstein, K.A. Semendjajew, G. Musiol, H. Mühlig, Taschenbuch der Mathematik, Harri Deutsch, Frankfurt/Main, Germany, 1993.
[32] C.D. Doyle, Estimating isothermal life from thermogravimetric data, J. Appl. Polym. Sci. 6 (1962) 639–642.
[33] A.W. Coats, J.P. Redfern, Kinetic parameters from thermogravimetric data, Nature 201 (1964) 68.
[34] V.M. Gorbachev, A solution of exponential integral in the nonisothermal kinetics for linear heating, J. Therm. Anal. Calorim. 8 (1975) 349–350.
[35] R.K. Agrawal, M.S. Sivasubramanian, Integral approximations for nonisothermal kinetics, J. Am. Chem. Eng. 33 (7) (1987) 1212–1214.
[36] J. Cai, F. Yao, W. Yi, F. He, New temperature integral approximation for nonisothermal kinetics, J. Am. Chem. Eng. 52 (4) (2006) 1554–1557.
[37] S. Vyazovkin, Computational aspects of kinetic analysis. Part C. The ICTAC Kinetics Project—the light at the end of the tunnel? Thermochim. Acta 355 (2000) 155–163.
[38] S. Vyazovkin, D. Dollimore, Linear and non-linear procedures in isoconversional computations of the activation energy of nonisothermal reactions in solids, J. Chem. Inf. Comput. Sci. 36 (1996) 42–45.
[39] S. Vyazovkin, A unified approach to kinetic processing of nonisothermal data, Int. J. Chem. Kinet. 28 (2) (1996) 95–101.
[40] W.S. Kohl, J. Frei, B.R. Trethewey, Characterization of the cure process in melamine–formaldehyde laminating resins using high-pressure differential scanning calorimetry, Tappi J. 79 (9) (1996) 199–205.
[41] S. Vyazovkin, W. Linert, Detecting isokinetic relationships in non-isothermal systems by the isoconversional method, Thermochim. Acta 269/270 (1995) 61–72.
[42] ASTM E 698, Standard Test Method for Arrhenius Constants for Thermally Unstable Materials, ASTM, Philadelphia, 1984.
[43] A. Kandelbauer, G. Wuzella, A. Mahendran, I. Taudes, P. Widsten, Using isoconversional kinetic analysis of liquid melamine–formaldehyde resin curing to predict laminate surface properties, J. Appl. Polym. Sci. 113 (4) (2009) 2649–2660.
[44] S. Vyazovkin, C.A. Wight, Estimating realistic confidence intervals for the activation energy determined from thermoanalytical measurements, Anal. Chem. 72 (2000) 3171–3175.
[45] P. Pourghahramani, E. Forssberg, Reduction kinetics of mechanically activated hematite concentrate with hydrogen gas using nonisothermal methods, Thermochim. Acta 454 (2007) 69–77.
[46] S. Vyazovkin, Model-free kinetics. Staying free of multiplying entities without necessity, J. Therm. Anal. Calorim. 83 (1) (2006) 45–51.